

Resonant photon tunneling via surface plasmon polaritons through one-dimensional metal-dielectric metamaterials

Satoshi Tomita^{1*}, Takashi Yokoyama¹, Hisao Yanagi¹, Ben Wood²,
John B. Pendry², Minoru Fujii³ and Shinji Hayashi³

¹ Graduate School of Materials Science, Nara Institute of Science and Technology (NAIST),
8916-5 Takayama, Ikoma, Nara 630-0192, Japan

² Blackett Laboratory, Imperial College London, Prince Consort Road, London SW7 2AZ,
United Kingdom

³ Graduate School of Engineering, Kobe University, Rokkodai 1-1, Nada, Kobe 657-8501,
Japan

tomita@ms.naist.jp

Abstract: We report resonant photon tunneling (RPT) through one-dimensional metamaterials consisting of alternating layers of metal and dielectric. RPT via a surface plasmon polariton state permits evanescent light waves with large wavenumbers to be conveyed through the metamaterial. This is the mechanism for sub-wavelength imaging recently demonstrated with a super-lens. Furthermore, we find that the RPT peak is shifted from the reflectance dip with increasing the number of Al layers, indicating that the shift is caused by the losses in the RPT.

© 2008 Optical Society of America

OCIS codes: (160.3918) Metamaterials; (240.6680) Surface plasmons; (240.7040) Tunneling.

References and links

1. D. R. Smith, J. B. Pendry, and M. C. K. Wiltshire, "Metamaterials and Negative Refractive Index," *Science* **305**, 788–792 (2004).
2. D. Schurig, J. J. Mock, B. J. Justice, S. A. Cummer, J. B. Pendry, A. F. Starr, and D. R. Smith, "Metamaterial Electromagnetic Cloak at Microwave Frequencies," *Science* **314**, 977–980 (2006).
3. V. M. Shalaev, "Optical negative-index metamaterials," *Nat. Photonics* **1**, 41–48 (2007).
4. S. A. Ramakrishna, J. B. Pendry, M. C. K. Wiltshire, and W. J. Stewart, "Imaging the near field," *J. Mod. Opt.* **50**, 1419–1430 (2003).
5. P. A. Belov and Y. Hao, "Subwavelength imaging at optical frequencies using a transmission device formed by a periodic layered metal-dielectric structure operating in the canalization regime," *Phys. Rev. B* **73**, 113110 (2006).
6. B. Wood, J. B. Pendry, and D. P. Tsai, "Directed subwavelength imaging using a layered metal-dielectric system," *Phys. Rev. B* **74**, 115116 (2006).
7. N. Fang, H. Lee, C. Sun, and X. Zhang, "Sub-Diffraction-Limited Optical Imaging with a Silver Superlens," *Science* **308**, 534–537 (2005).
8. Z. Liu, H. Lee, Y. Xiong, C. Sun, and X. Zhang, "Far-Field Optical Hyperlens Magnifying Sub-Diffraction-Limited Objects," *Science* **315**, 1686 (2007).
9. I. I. Smolyaninov, Y.-J. Hung, and C. C. Davis, "Magnifying Superlens in the Visible Frequency Range," *Science* **315**, 1699–1701 (2007).
10. I. Newton, *Opticks or A Treatise of the Reflections, Refractions, Inflections, and Colours of Light* (Dover Publications, New York, 1952), pp. 193–194, pp. 205–206.
11. R. Y. Chiao, P. G. Kwiat, and A. M. Steinberg, "Analogies between electron and photon tunneling: A proposed experiment to measure photon tunneling times," *Physica B* **175**, 257–262 (1991).

12. B. Lee and W. Lee, "TM-polarized photon tunneling phase time in a frustrated-total-internal-reflection structure," *J. Opt. Soc. Am. B* **14**, 777–781 (1997).
13. Y. Zhang, B. Fluegel, and A. Mascarenhas, "Total Negative Refraction in Real Crystals for Ballistic Electrons and Light," *Phys. Rev. Lett.* **91**, 157404 (2003).
14. H. Mizuta and T. Tanoue, *The Physics and Application of Resonant Tunneling Diodes* (Cambridge University Press, Cambridge, 1995).
15. A. Otto, "Calculations for an optical polarizer operating with frustrated total reflection," *Optik* **29**, 244–257 (1969).
16. A. Salwén and L. Stensland, "Spectral filtering possibilities of surface plasma oscillations in thin metal films," *Opt. Commun.* **2**, 9–13 (1970).
17. R. Dragila, B. Luther-Davies, and S. Vukovic, "High Transparency of Classically Opaque Metallic Films," *Phys. Rev. Lett.* **55**, 1117–1120 (1985).
18. S. Hayashi, H. Kurokawa, and H. Oga, "Observation of resonant photon tunneling in photonic double barrier structures," *Optical Rev.* **6**, 204–210 (1999).
19. I. Avrutsky, Y. Zhao, and V. Kochergin, "Surface-plasmon-assisted resonant tunneling of light through a periodically corrugated thin metal film," *Opt. Lett.* **25**, 595–597 (2000).
20. S. A. Darmanyany, and A. V. Zayats, "Light tunneling via resonant surface plasmon polariton states and the enhanced transmission of periodically nanostructured metal films: An analytical study," *Phys. Rev. B* **67**, 035424 (2003).
21. D. Gérard, L. Salomon, F. de Fornel, and A. V. Zayats, "Analysis of the Bloch mode spectra of surface polaritonic crystals in the weak and strong coupling regimes: grating-enhanced transmission at oblique incidence and suppression of SPP radiative losses," *Opt. Express* **12**, 3652–3662 (2004).
22. S. A. Darmanyany, M. Nevière, and A. V. Zayats, "Analytical theory of optical transmission through periodically structured metal films via tunnel-coupled surface polariton modes," *Phys. Rev. B* **70**, 075103 (2004).
23. L. Lin, R. J. Reeves, and R. J. Blaikie, "Surface-plasmon-enhanced light transmission through planar metallic films," *Phys. Rev. B* **74**, 155407 (2006).
24. B. Hou, H. Wen, Y. Leng, and W. Wen, "Enhanced transmission of electromagnetic waves through metamaterials," *Appl. Phys. A* **87**, 217–221 (2007).
25. I. R. Hooper, T. W. Preist, and J. R. Sambles, "Making Tunnel Barriers (Including Metals) Transparent," *Phys. Rev. Lett.* **97**, 053902 (2006).
26. E. D. Palik, *Handbook of Optical Constants of Solids* (Academic Press, 1997).
27. D. Y. Lei, and H. C. Ong, "Enhanced forward emission from ZnO via surface plasmons," *Appl. Phys. Lett.* **91**, 211107 (2007).

1. Introduction

Transporting photons between different locations is a central problem of the growing field of nanophotonics that is of critical importance for information processing and super-fine imaging. A door to such transportation of photons has recently been opened by electromagnetic metamaterials, which are assembled with artificial units smaller than the wavelength.[1, 2, 3] In particular, one-dimensional (1D) metamaterials consisting of alternating thin layers of metal and dielectric [4, 5, 6] are of great interest because of potential applications involving super-lenses, which enable us to go beyond the diffraction limit and obtain super-resolution images at optical frequencies.[7, 8, 9] The super-lensing effect is essentially based on resonant tunneling of photons with a large wavenumber.

The phenomenon of photon tunneling (PT) is originally found in literature by Newton.[10] Suppose a prism, which is made of glass with a high index of refraction (n_1), in the air. When a light wave in the prism enters the bottom of the prism at an incident angle (θ_i) above the critical angle of the total reflection [$\theta_c = \sin^{-1}(1/n_1)$], the propagating light wave is totally reflected at the interface between the prism bottom and air. However, the evanescent wave penetrates into the air and decays exponentially. Therefore, if another prism is placed near the bottom of the first prism, the evanescent wave reaches the second one and becomes propagating once more; the light thus passes through the air gap even if $\theta_i > \theta_c$. This is called PT, which is analogous to electron tunneling (ET) through a potential barrier in quantum mechanics. The phenomena of PT and ET are mathematically expressed in a similar way.[11, 12]

Analogy is sometimes helpful to understand a phenomenon and to expand a concept in

physics.[13] In the case of ET through a quantum well sandwiched between two potential barriers, the tunneling probability plotted as a function of the incident energy shows a peak when the energy matches that of a quasi-bound state inside the well; this is resonant ET.[14] A natural question arises: what is the photonic counterpart of resonant ET?

In the PT scheme mentioned above, let us insert a thin layer of metal, such as Al, Ag, or Au, into the air gap and replace the two separated air gaps with dielectric layers (index of refraction $n_2 < n_1$).[15, 16] The thin metal layer supports surface plasmon polaritons (SPPs), which (being non-radiative) can only be excited by evanescent waves of large wavenumber $k_x = (\omega/c)n_1 \sin \theta_{SPP}$ at the bottom of the incident prism at an angle of $\theta_i = \theta_{SPP} > \theta_c = \sin^{-1}(n_2/n_1)$. The SPPs convey the evanescent waves with large k_x to the other side of the metal. As a result, light tunnels through the metal layer via a resonant state of SPPs even if $\theta_i = \theta_{SPP} > \theta_c$ [17]; this is called resonant photon tunneling (RPT) [18]. RPT via a SPPs state is the basis for sub-wavelength imaging in a super-lens. Moreover, SPPs-assisted RPT has attracted much attention also from a view point of extraordinary high transmission of light through metal films with periodic sub-wavelength structures. [19, 20, 21, 22, 23, 24]

Dragila and co-workers [17] first demonstrated RPT in three-layer structures of $\text{MgF}_2/\text{Ag}/\text{MgF}_2$. RPT experiments in a similar system of $\text{SiO}_2/\text{Al}/\text{SiO}_2$ [18] and of $\text{ZnS}/\text{Ag}/\text{ZnS}$ [25] were also reported. These studies reveal RPT mechanism in three-layer structures containing a single metal layer, i.e., in photonic double barrier structures. However, little is known about RPT in alternating layers of metal/dielectric containing several numbers of metal layers (1D photonic metamaterials). In 1D photonic metamaterials mimicking an anisotropic material [6], evanescent waves of light with large k_x , which convey the sub-wavelength scale information of an object but which normally decay exponentially, can be carried for a long distance by RPT via coupled SPPs.[4]

In this paper, we report experimental and numerical studies on RPT through 1D metamaterials consisting of alternating Al/dielectric layers. In the experiment, we observed that evanescent light waves with large wavenumber can be carried through several Al layers in the metamaterials by the RPT via coupled SPPs. Furthermore, we found that the RPT peak is shifted from the reflectance dip with increasing the number of Al layers. With the help of numerical results, the origin of the shift is discussed.

2. Experimental

The alternating Al/dielectric multi-layers were prepared on a high refractive index glass (SFL11, index of refraction $n_1 = 1.778 + i0$ at 633 nm) substrate. (See inset in Fig. 1.) A coupling layer of SiO_2 ($n_2 = 1.457 + i0$ at 633 nm [26]) about 250 nm in thickness was deposited on the substrate using an rf-magnetron sputtering technique. Aluminium ($n_3 = 1.373 + i7.618$ at 633 nm [26]) and magnesium fluoride (MgF_2 , $n_4 = 1.377 + i0$ at 633 nm [26]) layers were alternatively deposited using a vacuum evaporation technique. The mass thickness of the Al and MgF_2 layers was monitored with a quartz crystal microbalance (QCM). The thickness of Al (d) is the same as that of MgF_2 . An SiO_2 decoupling layer, about 250 nm in thickness, was finally deposited using sputtering. The sample structure is represented by the number of Al layers, N , as $\text{SiO}_2/\text{Al}/[\text{MgF}_2/\text{Al}]_{N-1}/\text{SiO}_2$.

As illustrated in Fig. 1, a metamaterial sample was sandwiched between coupling and decoupling 60° prisms made of SFL11 using an index matching fluid (Methylene Iodide). A bare SFL11 substrate and an SFL11 substrate with only a 250 nm SiO_2 layer were simultaneously sandwiched as reference samples for transmission and reflection, respectively. The prisms with samples were mounted on one axis of a two-axis rotating stage. A He-Ne laser ($\lambda = 633$ nm) was used for a light source. p -polarization (p -pol) and s -polarization (s -pol) were switched using a half-wave plate. The reflected and transmitted light was detected with Si photo diodes. The an-

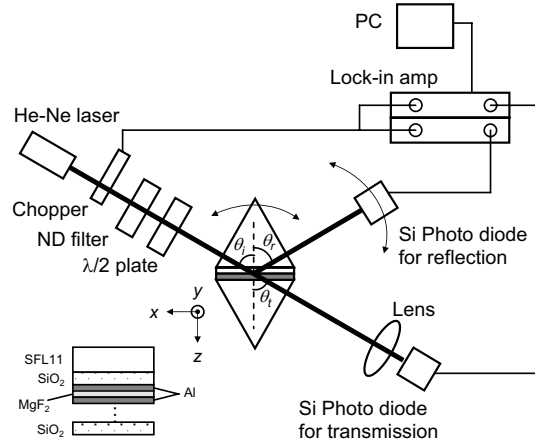


Fig. 1. Experimental setup for simultaneous photon reflection and tunneling measurements. Inset: a sample structure of a 1D alternating Al/dielectric metamaterial.

gle of the detector for tunneling (θ_t) was same as θ_i . The angle of the detector for reflection (θ_r) was always maintained at $\theta_r = \theta_i$ by the other axis of the stage. Before measurements, a 100 % transmission was measured through a bare SFL11 substrate at $\theta_i = 60^\circ$. At the same θ_i , a 100 % reflectance was also measured using the substrate with 250 nm SiO_2 because $\theta_c = 55^\circ$ at an interface between SFL11 and SiO_2 . Then, the intensities of reflected and transmitted (tunneled) light through a metamaterial sample were simultaneously recorded using lock-in amplifiers while changing θ_i . We refer to the reflectance spectra as the attenuated total reflection (ATR) spectra. We refer to the tunneling spectra as the PT spectra.

3. Results and discussion

Figure 2 shows the ATR (blue) and PT (red) spectra, which were simultaneously measured, for the $d = 40$ nm samples with (a) $N = 1$, (b) $N = 2$, and (c) $N = 3$. The horizontal axis corresponds to the incident angle in the coupling SFL11 prism (θ_i). The solid lines correspond to the p -pol and the dotted lines to the s -pol. The arrows show $\theta_c = 55^\circ$ at an interface between SFL11 and SiO_2 . In Fig. 2(a), the ATR spectrum exhibited a dip above θ_c with p -pol. On the other hand, no dips was observed with s -pol. These results suggest that the dip in the ATR spectrum with p -pol is caused by the excitation of SPPs in the Al layer because the SPPs are TM waves, which can be excited only with p -polarized light.

In the same figure, the PT spectrum with p -pol exhibits a peak at about $\theta_i = 56^\circ$, where the ATR spectrum shows a dip; this means that the light with a large k_x is tunneled. It is noticeable here that no peaks are observed with s -pol. This clearly show that the photon is resonantly tunneled via the SPPs through a single Al layer of 40nm in thickness. The maximum transmission at the RPT peak (T_{max}^{RPT}) around $\theta_i = 56^\circ$ was 58.64 %. This is an order of magnitude larger than the far-field transmittance at 633 nm (T_{633}^{Spe}) of 7.33 %, which is measured using a double-beam type UV-Vis spectrometer at normal incidence.

Figure 2(b) shows that photons tunneled through a sample with $N = 2$ although T_{max}^{RPT} becomes small: $T_{max}^{RPT} = 3.16$ %. (Note the value of the right vertical axis.) The corresponding T_{633}^{Spe} was 0.25 %. As shown in Fig. 2(c), we still observe RPT through an $N = 3$ sample containing three Al layers, for which the total mass thickness of Al ($d_{total}^{Al} = d \times N$) is equal to 120 nm. Although T_{max}^{RPT} is very small, $T_{max}^{RPT} = 0.21$ %, it is surprising because the transmittance with a UV-Vis spectrometer was undetectable and the samples seem to be just a mirror to the

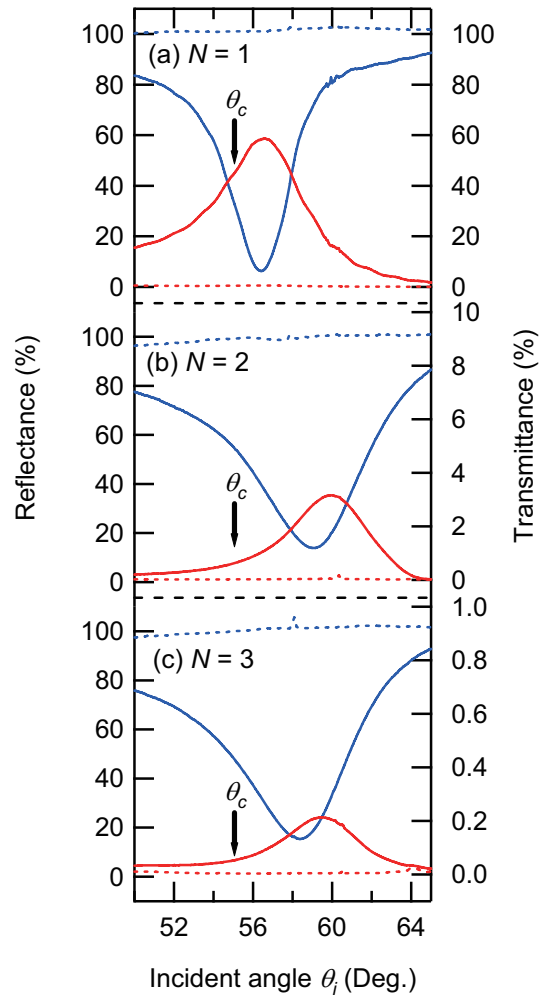


Fig. 2. Simultaneously measured ATR (blue) and PT (red) spectra of $d = 40$ nm samples with (a) $N = 1$, (b) $N = 2$, and (c) $N = 3$. Solid lines correspond to the p -pol and dashed lines to the s -pol. Arrows show $\theta_c = 55^\circ$ at an interface between SFL11 and SiO_2 .

eyes. The T_{max}^{RPT} observed in Fig. 2 and the corresponding T_{633}^{Spe} are summarized in Table 1. We see that T_{max}^{RPT} is an order of magnitude larger than T_{633}^{Spe} . In addition, it should be mentioned that an $N = 1$ sample containing a 120 nm Al layer did not exhibit a RPT peak (not shown here). This points out that chopping an opaque metal slab into several thin slices and using RPT via coupled SPPs improve transparency. The present results reveal that the near-field light with large k_x is efficiently conveyed by RPT with coupled SPPs through 1D metal/dielectric metamaterials. This is the basis for sub-wavelength imaging in a super-lens. [7, 8, 9]

Table 1. Experimental results for the $d = 40$ nm samples are summarized. The number of Al layers (N), the total mass thickness of Al ($d_{total}^{Al} = d \times N$), transmission maximum at RPT (T_{max}^{RPT}), far-field transmittance at 633nm measured using a UV-Vis spectrometer (T_{633}^{Spe}), and the shift variation ($\Delta\theta$).

N	d_{total}^{Al} (nm)	T_{max}^{RPT} (%)	T_{633}^{Spe} (%)	$\Delta\theta$ (°)
1	40	58.64	7.33	0.2
2	80	3.16	0.25	0.9
3	120	0.21	-	1.1

In Fig. 2, we notice that the position of the RPT peak (θ_{RPT}) is shifted rightward from that of the ATR dip (θ_{ATR}). The shift variation of the RPT peak ($\Delta\theta = \theta_{RPT} - \theta_{ATR}$) in the $d = 40$ nm sample is summarized in Table 1. $\Delta\theta$ increases with N . To reveal the origin of the shift, we carried out numerical simulations using the 2×2 transfer matrix method. Figure 3 shows calculated ATR (blue) and PT (red) spectra of a metamaterial with $d = 40$ nm with (a) $N = 1$, (b) $N = 2$, and (c) $N = 3$, which corresponds to Fig. 2. The solid lines correspond to the p -pol and the dotted lines to the s -pol. An index of refraction of Al described in the Experimental section ($n_3 = 1.373 + i7.618$) is used. ATR dip and RPT peak are clearly seen for p -pol; the numerical simulation reproduces the experimental results. There is some movement of the transmission peak. The RPT in the simulation peak is shifted rightward with increasing N , as found in the experiments, although the peak position is somewhat different between experiment and simulation. This discrepancy is considered to be caused by the difference in thickness and index of refraction of dielectric SiO_2 and MgF_2 . In Fig. 4, $\Delta\theta$ observed in the experiments for samples with $d = 40$ and 30 nm is plotted as a function of N (solid squares). In the same figure, simulated $\Delta\theta$ is also plotted for various d from $d = 10$ to 40 nm (crosses). The figure shows that $\Delta\theta$ both in experiments and calculation increases with an increase in N except for $d = 10$ nm in numerical simulation.

An increase in N brings about an increase in the intrinsic losses in Al layers of metamaterials due to the imaginary part of refractive index. One of the origins for the $\Delta\theta$ is thus the intrinsic losses in the system. We carried out calculations using the refractive index of Al multiplied by 0.8 ($n_3' = 1.098 + i6.094$). Open circles in Fig. 4 correspond to the calculated $\Delta\theta$. A smaller refractive index causes a smaller $\Delta\theta$. Moreover, $\Delta\theta$ is almost zero in an RPT via a guided mode through alternating dielectric/dielectric multilayers without intrinsic losses (not shown here).

Even though an increase in measured $\Delta\theta$ with N agrees qualitatively with simulation results, there are quantitatively some differences. The measured $\Delta\theta$ is much larger than the calculated ones. In addition, calculated $\Delta\theta$ becomes negative for $N = 1$ samples. Therefore, there is an additional origin for the shift, which is related to the losses. For example, the extrinsic losses due to scattering at the interfaces between Al and dielectric layers is possible. In experiment, we observed a consequence of the combination of both origins.

When the ATR spectra in Fig. 2 show dips at incident angles of $\theta_i = \theta_{ATR}$, the SPPs are excited in Al layers in the metamaterials. The resonance with the SPPs leads to an electric field enhancement of light. The RPT exhibits a peak at an incident angle of $\theta_i = \theta_{RPT}$, where the

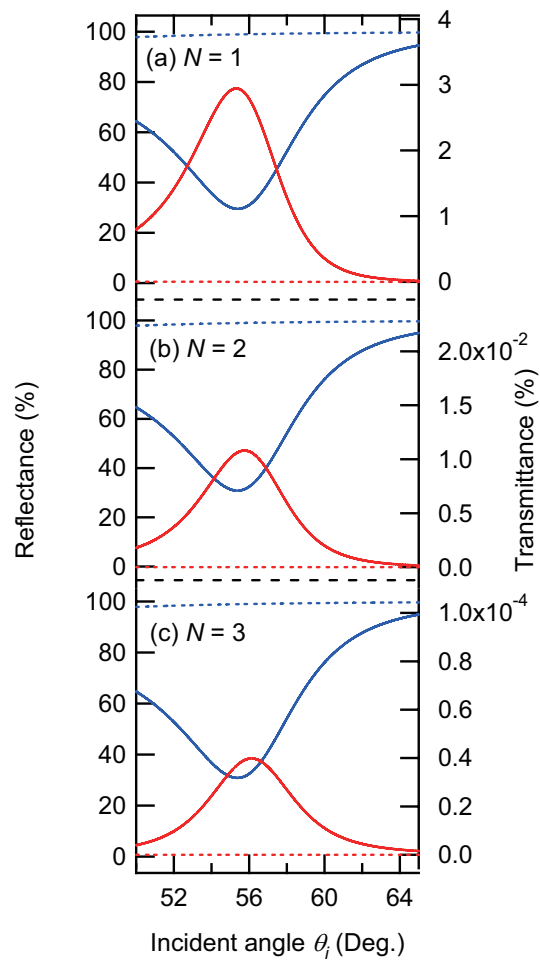


Fig. 3. Numerically simulated ATR (blue) and PT (red) spectra of $d = 40$ nm samples with (a) $N = 1$, (b) $N = 2$, and (c) $N = 3$. Solid lines correspond to the p -pol and dashed lines to the s -pol.

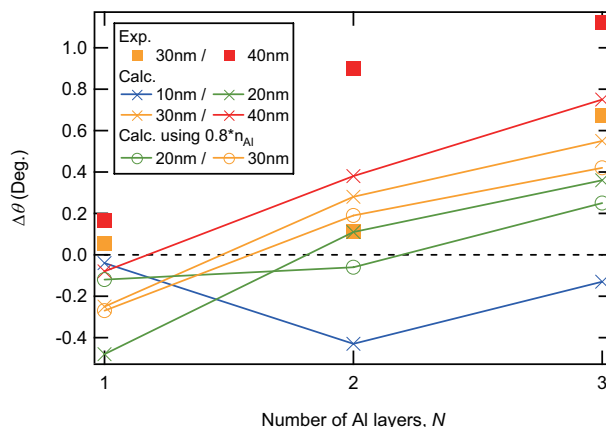


Fig. 4. Shift variation of the RPT peak from the reflection dip ($\Delta\theta$) for various d is plotted as a function of number of Al layers, N . Solid squares are assigned to experimental results. Crosses correspond to the numerical results using refractive index of Al described in the Experimental section. Open circles also correspond to the numerical results but using the refractive index of Al multiplied by 0.8.

electric field is most enhanced. The shift variation ($\Delta\theta$) of the RPT peak from the ATR dip thus corresponds to a difference between incident angles for the greatest field enhancement by the SPPs resonance (θ_{RPT}) and for the excitation of SPPs (θ_{ATR}): $\Delta\theta = \theta_{RPT} - \theta_{ATR}$. The present results indicate that an increase in N , i.e., a coupling of SPPs through the metal/dielectric multilayers, enhances a difference in incident angles for the greatest field enhancement by the SPPs resonant from that for the excitation of SPPs.

Comparing the measured spectra in Fig. 2 and calculated spectra in Fig. 3, we find that the transmittance in calculations is much lower than that in measurements. Figure 5 shows transmission maximum at a RPT peak for samples with various d as a function of N . Solid squares correspond to experimental results. Crosses correspond to the calculation results using $n_3 = 1.373 + i7.618$ for Al. For both $d = 30$ nm and 40 nm, the transmission maximum in the calculations is much lower than that in the experiments. From the fabrication point of view, it is plausible that the thickness of Al and MgF_2 is not exact the same as the values monitored using a QCM. In addition, index of refraction for Al is known to depend strongly on the deposition condition. Open circles in Fig. 5 correspond to the transmission maximum calculated using a smaller index of refraction for Al ($n'_3 = 1.098 + i6.094$). The measured transmittance maximum with $d = 40$ nm is very similar with the calculated one with $d = 20$ nm and $n_3 = 1.373 + i7.618$, or with $d = 30$ nm and $n'_3 = 1.098 + i6.094$.

In addition to the difference in thickness or refractive index of Al, we note here a possible enhanced transmission of light by the roughness at an interface between Al and dielectrics. As already mentioned in the Introduction, Avrutsky and co-workers [19] presented extraordinary transmission of light with a periodically corrugated thin metal film, which can be treated as surface-plasmon-enhanced resonant tunneling of light through a metal film with grating. The sample is similar to the sample with $N = 1$ in the present study, although we do not introduce a periodic corrugation. Lie and Ong [27] reported that the measured transmission in Al/dielectric/Al/ZnO, which is similar to the sample with $N = 2$ in the present study, is one order of magnitude higher than the calculated one. They attribute this discrepancy to the thickness inhomogeneity and roughness in the multilayer structures as well as the uncertainty in the dielectric constants of Al. Therefore, the transmittance in the present photon tunneling

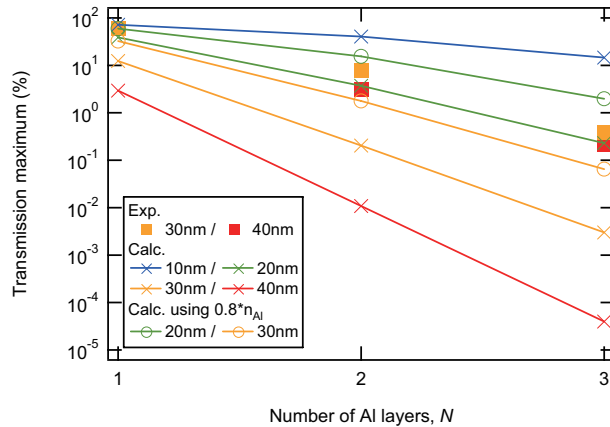


Fig. 5. Measured and calculated transmission maximum for various d is plotted as a function of number of Al layers, N .

experiments may be enhanced by the thickness inhomogeneity and roughness at interfaces between Al and dielectrics.

4. Conclusion

In conclusion, RPT in 1D metamaterials consisting of alternating Al/dielectric layers has been studied. We have succeeded in observing experimentally that evanescent waves with large wavenumbers can be carried through several Al layers in the metamaterials by the RPT via coupled SPPs. This SPPs-mediated transmission is an order of magnitude larger than the transmission for light at normal incidence. Moreover, the measured SPPs-mediated transmission is much larger than the calculated one. This discrepancy is primarily caused by the uncertainty in thickness or the refractive index of Al. In addition, the transmittance may be enhanced by the roughness at interfaces between Al and dielectrics. The present results show that slicing an opaque metal slab into several thin layers and using RPT make the metal semi-transparent, demonstrating the mechanism used in sub-wavelength imaging by a super-lens. We also found a shift of the RPT peak from the ATR dip, which was reproduced by numerical simulation. This originates from the losses due to heating in the metal and scattering at the layer boundaries.

Acknowledgments

The authors thank T. Nakamura, S. Miura, S. Hayashi and A. Ishizumi for valuable discussions. ST acknowledges Japan-U.K. Nanoscience & Technology Young Scientists Exchange Program and Grant-in-Aid for Scientific Research (No. 19710081) from the MEXT, Japan.